SCIENTIFIC REPORTS

OPEN

SUBJECT AREAS:
NANOSCALE MATERIALS
MATERIALS FOR DEVICES

Received
1 April 2014

Accepted
6 June 2014

Published
27 June 2014

Correspondence and requests for materials should be addressed to X.X. (xiaxiang@uestc.edu.cn); L.Q. (qiaol@ornl.gov) or S.L. (sean.li@unsw.edu.au)

Effects of surface defects on two-dimensional electron gas at $NdAlO_3/SrTiO_3$ interface

X. Xiang[1], L. Qiao[2], H. Y. Xiao[1], F. Gao[3], X. T. Zu[1], S. Li[4] & W. L. Zhou[5]

[1]School of Physical Electronics, University of Electronic Science and Technology of China, Chengdu 610054, China, [2]Center for Nanophase Materials Sciences, Oak Ridge National Laboratory, Oak Ridge, TN, USA, [3]Pacific Northwest National Laboratory, P.O. Box 999, Richland, WA 99352, USA, [4]School of Material Science and Engineering, University of New South Wales, Sydney, 2052, Australia, [5]Advanced Materials Research Institute, University of New Orleans, New Orleans, LA, 70148, USA.

Density functional theory calculations of $NdAlO_3/SrTiO_3$ heterostructure show that two-dimensional electron gas (2-DEG) is produced at the interface with a built-in potential of ~0.3 eV per unit cell. The effects of surface defects on the phase stability and electric field of 2-DEG have been investigated. It is found that oxygen vacancy is easily to form on the $NdAlO_3$(001) surface, with a low threshold displacement energy and a low formation energy. This point defect results in surface reconstruction and the formation of a zigzag -Al-O-Al- chain, which quenches the built-in potential and enhances the carrier density significantly. These results will provide fundamental insights into understanding how surface defects influence the electronic behavior of 2-DEG and tuning their electronic properties through surface modification.

With the breakthrough of cutting-edge thin-film epitaxial techniques like pulsed laser deposition and molecular-beam epitaxy, high quality heterointerfaces based on perovskite transition metal oxides have been achieved experimentally and revealed to exhibit a large number of fascinating electrical and magnetic properties[1]. A prominent example is the discovery of the two-dimensional electron gas (2-DEG) at the interface between two band insulators, polar $LaAlO_3$ (LAO) and non-polar $SrTiO_3$ (STO)[2]. Due to its intriguing functionalities[3–5], unparalleled environmental stabilities over traditional semiconductors, and capability for nanoscale read/write/erase[6], as well as field-effect transistor and non-volatile memory effects, oxide heterostructures are now considered as promising candidates for breeding next-generation high-performance electronics and spintronics.

In recent years, the origin of the 2-DEG formation at the LAO/STO(001) interface has attracted broad interests[7,8]. Along the [001] direction STO is composed of neutral layers $(SrO)^0$ and $(TiO_2)^0$, and LAO consists of alternately charged atomic layers $(LaO)^+$ and $(AlO_2)^-$. Electronic reconstruction can occur near the electron-rich n-type LaO/TiO_2 interface to avoid the polarization catastrophe caused by the diverging Coulomb field[9–12]. On the other hand, oxygen vacancies created during the deposition process can dope electrons in STO substrate and induce the interface conductivity[13,14].

Cation nonstoichiometry and intermixing at the interface[15–18] have also been proposed to result in the conducting interface. To investigate the role of the ABO_3 polar layer and explore 2-DEG with higher carrier density and hole mobility, various perovskite oxide thin films on STO substrate, e.g., $NdAlO_3$[19], $GdTiO_3$[20], $LaMnO_3$[21], $LaGaO_3$[22,23], and $LaCrO_3$[24], have been studied. Recently, Annadi *et al.* reported that $NdAlO_3/SrTiO_3$ (NAO/STO) can also produce 2-DEG at the interface that exhibits a stronger localization of 2-DEG than LAO/STO interfaces[19,25]. However, there is a lack of theoretical understanding of the formation mechanism.

In the potential application of 2-DEG as electronic devices in aerospace industries, surface defects may be created due to radiation in a harsh environment. Knowledge of radiation response, surface defect stability and its influence on 2-DEG behavior are thus of vital importance for realistic applications. This is also important for surface modification by ion beam implantation[26] to improve overall performance of future electronic devices under harsh environments and to design novel materials with enhanced performance. In spite of the studies on the stabilities of the intrinsic defects on surface or at interfaces[27–30], very few experimental and theoretical investigations of heterostructures under irradiation have been reported. In this work, a first-principles study of the $NdAlO_3/SrTiO_3$(001) heterointerface is carried out to explore its low energy radiation response and the stability of the built-in potential with respect to surface defect formation. Our results reveal that the surface

oxygen within the NAO/STO heterostructure can be easily displaced, which reduces the built-in potential to zero, and enhances the carrier density significantly. However, the surface aluminum vacancy formation is hard to form, and its formation energy is relatively high, independent of the thickness of NAO, and is shown to sustain the built-in potential.

The first-principles calculations are performed within the density functional theory (DFT) framework using the projector augmented wave method, as implemented in the Vienna Ab Inito Simulation Package (VASP)[31]. The exchange-correlation effects are treated by the generalized-gradient approximation (GGA) in the Perdew-Burke-Ernzerhof parametrization[32], with spin-polarized effects considered. A plane-wave cutoff energy of 400 eV and a $4 \times 4 \times 1$ k-point sampling in Brillouin zone are used. Slab models for $(NAO)_n/(STO)_4$ (n=2, 4, 6, 8, and 10), in which one slab consisting of n layers of NAO and four layers of STO, and a vacuum region of 15 Å separating the periodically repeated slabs, are employed in the calculations. A $\sqrt{2} \times \sqrt{2}$ unit cell is taken into account. We only consider the n-type interface, which is formed by a layer sequence of …-(SrO)-(TiO_2)-(NdO)-(AlO_2)-…. The surface of the NAO overlayer is AlO_2 terminated. The geometry of the simulation cell for $(NAO)_4/(STO)_4$ is shown in Fig. 1(a). The two-dimensional lattice parameters are fixed at 3.94 Å, which is the optimized lattice constant for the bulk STO. Structural optimization is carried out in the condition that the Hellmann–Feynman force on each atom is smaller than 0.01 eV $Å^{-1}$. The dipole correction is applied to remove the undesired electrostatic interaction between periodic cells along the direction perpendicular to the surface. Correlation effect[33] has been tested and it is shown that the obtained results are very similar to those without considering this effect.

The total density of states for 2–4 layers of NAO film on STO(001) presented in Fig. 1(b) show that $(NAO)_2/(STO)_4$ owns a band gap as small as 0.6 eV. The band gap, defined by occupied O 2*p* states at the surface and unoccupied Ti 3*d* states at the interface, decreases with increasing thickness of the NAO film and a crossover to an insulator-to-metal transition occurs for thin film thickness between 3 and 4 unit cells (u.c.). Experimentally it is also observed that a transition from insulating to metallic interface occurs at a thickness around 4 u.c[19]. Such agreement is surprising since our GGA calculations underestimate the band gap of STO by 1.95 eV and the critical thickness should increase by around two layers when the valence-band offset at the interface is correctly described within GGA and the true energy gap of STO is considered[34]. There is a possibility that the true valence-band offset is very different from the GGA results such that the energy gap underestimation is effectively cancelled by the error in the valence-band offset[34]. Layer-resolved density of states for $(NAO)_4/(STO)_4$ interface is presented in Fig. 2(a). It is shown that the valence edge in NAO, which is mainly contributed by O 2*p* in the surface AlO_2 layer, increases linearly in energy with the distance from the interface. This built-in potential (~0.3 eV/u.c.) results in the emergence of a small concentration of charge carrier, i.e., holes at the top NAO layer and electrons that spread over several STO layers, supporting the idea that electronic reconstruction could be the driving mechanism for the creation of the 2-DEG at the interfaces[9–11]. It is found that NAO/STO heterointerface exhibits similar characteristics in the insulator-metal transition and the thickness dependency of the polar layer to LAO/STO system[10,34].

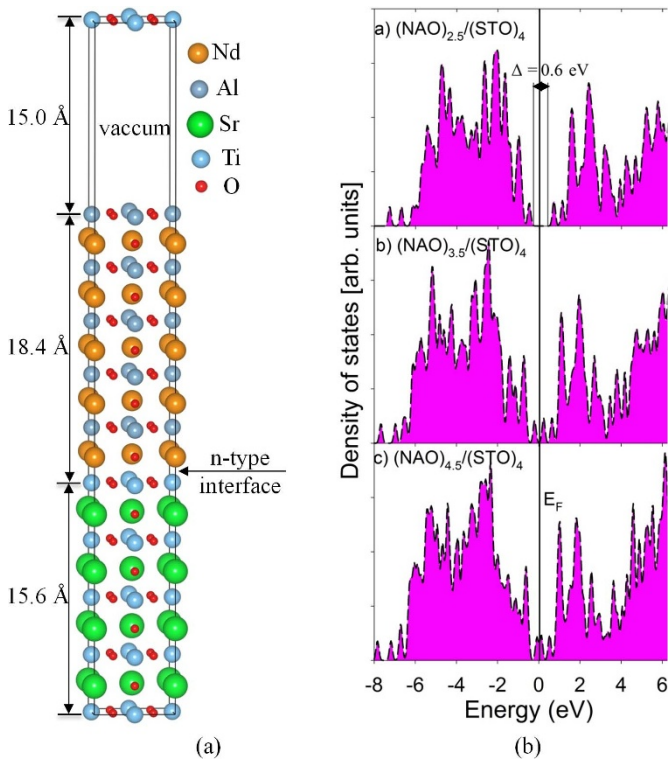

Figure 1 | (a) Structural model for $(NAO)_4/(STO)_4$ and (b) total density of states of $(NAO)_n/(STO)_4$, where the Fermi level E_F is set to zero.

To investigate the low energy radiation response of NAO/STO heterostructure, the threshold displacement energies (E_d) of surface atoms are calculated. Threshold displacement energy is defined as the minimum amount of transferred kinetic energy necessary to permanently displace an atom from its original lattice site, thus, forming a stable defect[35]. This physical parameter is important for determining the primary state of radiation damage in a material and estimating the total amount of damage states created under ion irradiation[36–38]. Along the direction perpendicular to the surface, the E_d are calculated to be 9 eV for surface oxygen and 40 eV for surface aluminum, which correspond to electron irradiation of 60 and 360 KeV, respectively. The respective created defects are mainly surface oxygen vacancy and aluminium vacancy. The low E_d value of 9 eV for surface oxygen indicates that it is easily to be displaced and surface oxygen vacancies will be one of the dominant defects under irradiation. In order to study the stability of surface defects in NAO/STO heterostructure, one oxygen or aluminum is removed from the surface, and the formation energies for surface oxygen vacancy and aluminum vacancy are calculated. The formation energy is defined by $E_f = E_{def} - E_{perf} + \mu_i$[29]. Here E_{def} and E_{perf} are the total energies for defective and perfect heterostructures, respectively. The μ_i is the chemical potential of oxygen or aluminum, which is obtained under O-rich condition[39]. The defect formation energies as a function of NAO layers are provided in Fig. 3(a). It should be pointed out that the variation of defect formation energy with thin film thickness is independent of the oxygen or Al chemical potential. As shown in the figure, the formation of surface oxygen vacancy becomes easier with increasing NAO thin film thickness. This is consistent with the theoretical calculations of LAO/STO performed by Zhang *et al.*[29] However, the formation of surface Al vacancy shows negligible dependence on the thin film thickness. It is also found that the formation energy for surface Al vacancy is much higher than that for surface O vacancy, confirming the finding that surface oxygen vacancies will be one of the dominant defects under irradiation.

The vertical displacement in the NAO layers for an ideal $(NAO)_4/(STO)_4$ and the heterointerfaces with surface oxygen or aluminum defects is investigated in Fig. 3(b) and 3(c). For the ideal $(NAO)_4/(STO)_4$ structure, it is noted that Nd relaxes outward by 0.10–0.22 Å and the Nd far from the interface shows the largest relaxation of 0.22 Å. On the other hand, the displacement of Al is small and the surface Al only shifts inward by 0.05 Å. Oxygen ions in NdO and AlO_2 layers relaxes inward by 0.01–0.05 Å and 0.02–0.12 Å, respectively. This large polar distortion has a remarkable impact on the electronic behavior of the heterostructures and results in electronic

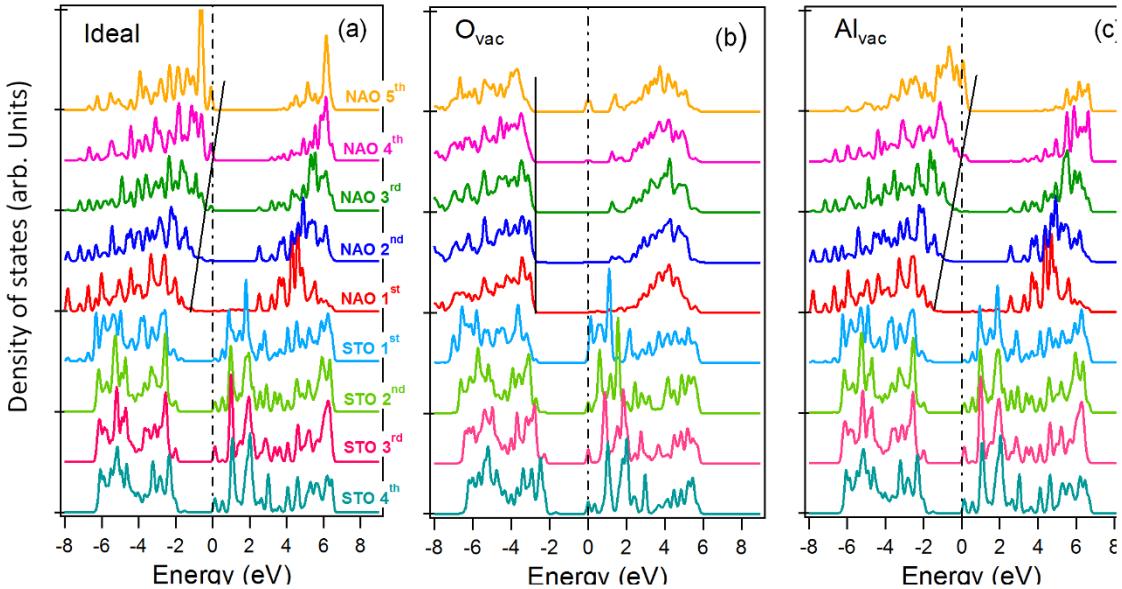

Figure 2 | **Layer-resolved density of states for (a) ideal $(NAO)_4/(STO)_4$ interface; (b) interface with surface oxygen vacancy; (c) interface with surface aluminum vacancy, where the Fermi level E_F is set to zero.**

reconstruction. The polar-type distortion in NdO layers is very similar to that in LaO layers of LAO/STO heterointerfaces[10]. The introduction of surface O vacancy is shown to have slight influences on the vertical displacement of ions in NdO and AlO_2 layers. When oxygen vacancy exists on the surface, NdO layers show small relaxation of 0.04–0.06 Å. The surface and subsurface AlO_2 layers are found to exhibit different features, i.e., surface AlO_2 layer relaxes inward by 0.07 Å, while subsurface AlO_2 layers relax outward by 0.05 Å. The most striking result for NAO/STO heterostructure with surface O vacancy is that oxygen ions in NdO layers have large in-plane dis-

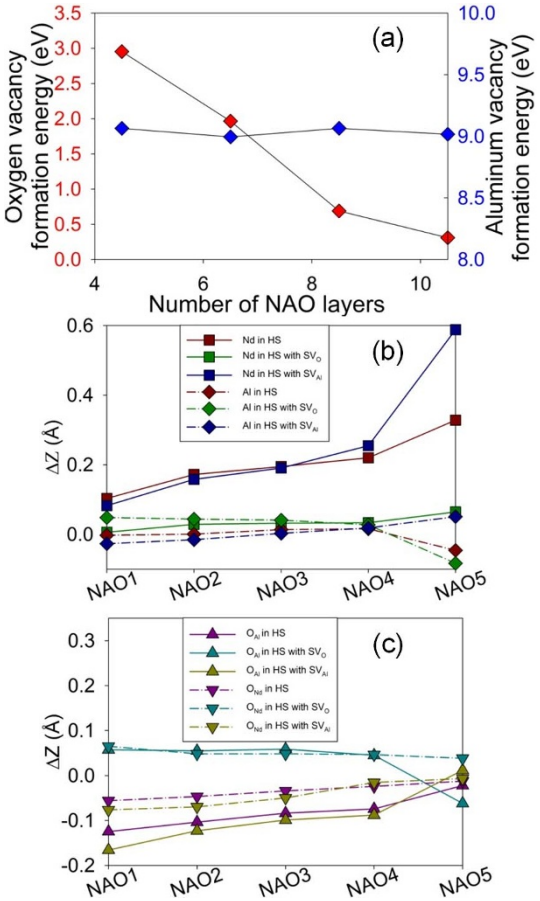

Figure 3 | **(a) Variation of vacancy formation energy with thin film thickness; (b) vertical displacements of cations in the NAO layers for $(NAO)_4/(STO)_4$, and (c) vertical displacements of anions in the NAO layers for $(NAO)_4/(STO)_4$.**

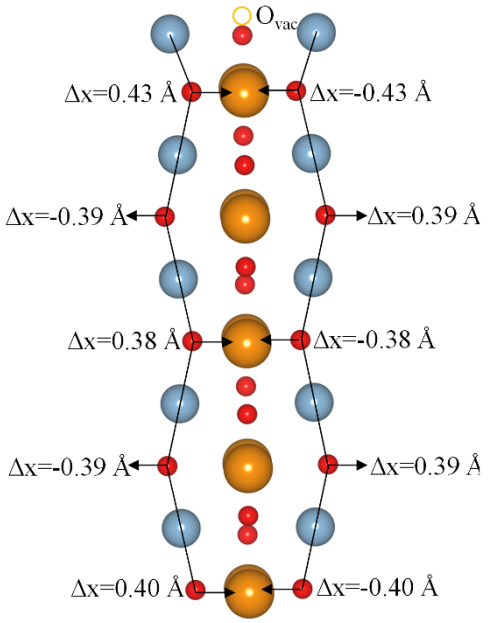

Figure 4 | Illustration of optimized geometrical configuration for $NdAlO_3$ thin film with surface oxygen vacancy, where the atom representations are the same as those in Fig. 1(a).

placements. According to Fig. 4, the oxygen ions in the NdO layers are displaced by 0.40 Å from their ideal lattice sites. This displacement exhibits a compression and expansion behavior alternately, forming a zigzag -Al-O-Al- chain structure which has also been observed experimentally in LAO/STO interface[40]. Cen et al. have performed first-principles density functional theory calculations of LAO films on STO substrates, and a zigzag –Al-O-Al chian structure is also found when oxygen ions are removed from the LAO surface layer[41]. In addition, the large distortion is expected to significantly affect the built-in potential and electronic properties of heterostructures. For a NAO/STO heterostructure with surface Al vacancy, the optimized structure shows nearly zero in-plane displacement. This phenomenon is different from the case of surface O vacancy, but it is very similar to that of an ideal NAO/STO. Vertically, the ions in different NAO overlayers are also found to relax in a similar way to that in ideal NAO/STO. Nevertheless, the Nd ions farthest from the interface are found to have larger outward relaxation of 0.59 Å, as compared with the value of 0.33 Å in an ideal NAO/STO structure. Another difference is that the surface Al shifts outward and inward in the defective and ideal heterostructure, respectively. The electronic properties for NAO/STO with surface Al vacancy are thus expected to be similar to those for ideal states.

To explore the built-in potential stability with respect to vacancy defects, the layer-resolved density of states for defective heterostructure are compared with those for ideal states in Fig. 2. It is of interest to find that the surface oxygen vacancy causes significant electron redistribution and the built-in potential vanishes. This is because the formation of surface oxygen vacancy in the AlO_2 layer introduces two excess electrons, which interact with the extra holes near the valence band maximum. The Coulomb coupling between the oxygen vacancy donor and the host results in charge transfer and hole compensation. This effect reduces the polarization of the NAO overlayer, indicating that the carrier density will be increased and the conductivity at the interface will be enhanced. In contrast, a neutral Al vacancy at the AlO_2 surface would produce three holes and leaving the overall charge unchanged. The tilt of the NAO band structure due to the built-in potential is thus sustained because the AlO_2 surface charge cannot be compensated by Al vacancy.

By adding the occupation numbers of the states corresponding to the electrons transferred from NAO to STO, the carrier density in STO can be obtained. Fig. 5 presents the variation of carrier densities with thin film thickness for ideal and defective NAO/STO. In all cases, it is found that the carrier density increases with the thin film thickness. Annadi *et al.* also observed that at low temperatures below 20 K down to 2 K the carrier density increases as the NAO thickness increases from 6 to 12 u.c[25]. This is because with increasing NAO thickness the local valence band maximum of NAO in the surface region rises more above the conduction band minimum of STO, which results in larger charge transfer from NAO to STO and smaller electric filed inside NAO. For a 6 u.c. thin film, the carrier density is predicted to be 1.85×10^{14} electrons/cm^2, which is larger than the experimental value of 0.53×10^{14} electrons/cm^2. Similar phenomenon has also been observed in LAO/STO system[34]. In the case of NAO/STO with surface oxygen vacancy, the carrier density is enhanced significantly as compared with the ideal states, due to the reduced built-in potential. Surface aluminum vacancy, on the other hand, lowers the density slightly because the introduced holes in the surface area lead to less electrons transferring from NAO to STO. These results suggest that the electronic behavior is influenced significantly under radiation environment and the surface of heterostructure can be modified by introduction of defects.

In summary, first-principles calculations show that two-dimensional electron gas can be produced at NAO/STO(001) heterointerface with a critical thickness of 3 ~ 4 u.c. The threshold displacement energies for surface O and Al are determined to be 9 and 40 eV, respectively, and the formation energy for a surface Al vacancy is much higher than that for a surface O vacancy, suggesting that the heterointerface is susceptible to irradiation and oxygen vacancy is one of the dominant defects. Surface Al vacancy is found to have minimal effects on the built-in potential in NAO/STO, while surface oxygen vacancy reduces the potential to zero due to surface reconstruction and the formation of a zigzag -Al-O-Al- chain. The holes introduced by surface aluminum vacancy lead to less electrons transferring from NAO to STO and lower the carrier density slightly; however, the excess electrons introduced by surface oxygen vacancy compensate the holes at the surface and enhance the carrier density significantly. These results provide an important understanding of radiation effects on the heterostructures, which is a necessity for achieving radiation-resistant electronic devices based on oxide 2-DEG through manipulating the electronic surface properties.

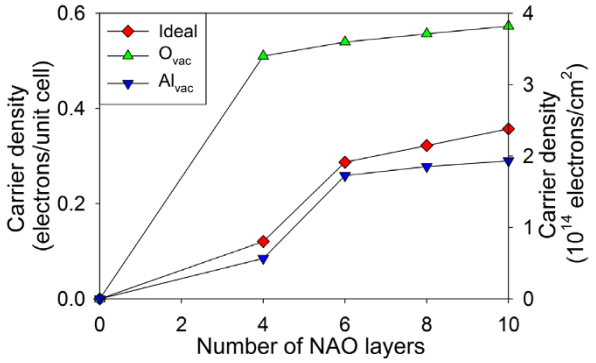

Figure 5 | Variation of carrier densities with thin film thickness for ideal and defective NAO/STO. The O_{vac} and Al_{vac} represent oxygen and aluminum vacancy, respectively.

1. Mathew, S. *et al.* Tuning the Interface Conductivity of LaAlO3/SrTiO3 Using Ion Beams: Implications for Patterning. *ACS Nano* **7**, 10572 (2013).
2. Ohtomo, A. & Hwang, H. Y. A high-mobility electron gas at the LaAlO3/SrTiO3 heterointerface. *Nature* **427**, 423 (2004).
3. Popovic, Z. S. & Satpathy, S. Wedge-Shaped Potential and Airy-Function Electron Localization in Oxide Superlattices. *Phys. Rev. Lett.* **94**, 176805 (2005).

4. Brinkman, A. *et al.* Magnetic effects at the interface between non-magnetic oxides. *Nature Mater.* **6**, 493 (2007).
5. Reyren, N. *et al.* Superconducting Interfaces Between Insulating Oxides. *Science* **317**, 1196 (2007).
6. Cen, C. *et al.* Nanoscale control of an interfacial metal–insulator transition at room temperature. *Nature Mater.* **7**, 298 (2008).
7. Liu, Z. Q. *et al.* Origin of the Two-Dimensional Electron Gas at LaAlO3=SrTiO3 Interfaces: The Role of Oxygen Vacancies and Electronic Reconstruction. *Phys. Rev. X* **3**, 021010 (2013).
8. Yoshimatsu, K., Yasuhara, R., Kumigashira, H. & Oshima, M. Origin of Metallic States at the Heterointerface between the Band Insulators LaAlO3 and SrTiO3. *Phys. Rev. Lett.* **101**, 026802 (2008).
9. Nakagawa, N., Hwang, H. Y. & Muller, D. A. Why some interfaces cannot be sharp. *Nature Mater.* **5**, 204 (2006).
10. Pentcheva, R. & Pickett, W. E. Avoiding the Polarization Catastrophe in LaAlO3 Overlayers on SrTiO3(001) through Polar Distortion. *Phys. Rev. Lett.* **102**, 107602 (2009).
11. Popović, Z. S., Satpathy, S. & Martin, R. M. Origin of the Two-Dimensional Electron Gas Carrier Density at the LaAlO3 on SrTiO3 Interface. *Phys. Rev. Lett.* **101**, 256801 (2008).
12. Harrison, W. A., Kraut, E. A., Waldrop, J. R. & Grant, R. W. Polar heterojunction interfaces. *Phys. Rev. B* **18**, 4402 (1978).
13. Pavlenko, N., Kopp, T., Tsymbal, E. Y., Mannhart, J. & Sawatzky, G. A. Oxygen vacancies at titanate interfaces: Two-dimensional magnetism and orbital reconstruction. *Phys. Rev. B* **86**, 064431 (2012).
14. Pavlenko, N., Kopp, T., Tsymbal, E. Y., Sawatzky, G. A. & Mannhart, J. Magnetic and superconducting phases at the LaAlO3/SrTiO3 interface: The role of interfacial Ti 3d electrons. *Phys. Rev. B* **85**, 020407(R) (2012).
15. Willmott, P. R. *et al.* Structural Basis for the Conducting Interface between LaAlO3 and SrTiO3. *Phys. Rev. Lett.* **99**, 155502 (2007).
16. Qiao, L., Droubay, T. C., Kaspar, T. C., Sushko, P. V. & Chambers, S. A. Cation mixing, band offsets and electric fields at LaAlO3/SrTiO3(001) heterojunctions with variable La:Al atom ratio. *Surf. Sci.* **605**, 1381 (2011).
17. Qiao, L. *et al.* Epitaxial growth, structure, and intermixing at the LaAlO3/SrTiO3 interface as the film stoichiometry is varied. *Phys. Rev. B* **83**, 085408 (2011).
18. Warusawithana, M. P. *et al.* LaAlO3 stoichiometry is key to electron liquid formation at LaAlO3/SrTiO3 interfaces. *Nat. Commun.* **4**, 2351 (2013).
19. Annadi, A. *et al.* Electronic correlation and strain effects at the interfaces between polar and nonpolar complex oxides. *Phys. Rev. B* **86**, 085450 (2012).
20. Boucherit, M. *et al.* Extreme charge density SrTiO3/GdTiO3 heterostructure field effect transistors. *Appl. Phys. Lett.* **102**, 242909 (2013).
21. Barriocanal, J. G. *et al.* "Charge Leakage" at LaMnO3/SrTiO3 Interfaces. *Adv. Mater.* **22**, 627 (2010).
22. Nazir, S., Amin, B. & Schwingenschlogl, U. Suppression of the two-dimensional electron gas in LaGaO3/SrTiO3 by cation intermixing. *Sci. Rep.* **3**, 3409 (2013).
23. Nazir, S., Singh, N. & Schwingenschlogl, U. The metallic interface between the two band insulators LaGaO3 and SrTiO3. *Appl. Phys. Lett.* **98**, 262104 (2011).
24. Chambers, S. A. *et al.* Band Alignment, Built-In Potential, and the Absence of Conductivity at the LaCrO3/SrTiO3(001) Heterojunction. *Phys. Rev. Lett.* **107**, 206802 (2011).
25. Annadi, A. *et al.* Evolution of variable range hopping in strongly localized two dimensional electron gas at NdAlO3/SrTiO3 (100) heterointerfaces. *Appl. Phys. Lett.* **101**, 231604 (2012).
26. Zhu, S., Wang, L. M., Zu, X. T. & Xiang, X. Optical and magnetic properties of Ni nanoparticles in rutile formed by Ni ion implantation. *Appl. Phys. Lett.* **88**, 043107 (2006).
27. Gu, M. Q., Wang, J. L., Wu, X. S. & Zhang, G. P. Stabilities of the Intrinsic Defects on SrTiO3 Surface and SrTiO3/LaAlO3 Interface. *J. Phys. Chem. C* **116**, 24993 (2012).
28. Seo, H. & Demko, A. A. First-principles study of polar LaAlO3(001) surface stabilization by point defects. *Phys. Rev. B* **84**, 045440 (2011).
29. Zhang, L. *et al.* Origin of insulating behavior of the p-type LaAlO3/SrTiO3 interface: Polarization-induced asymmetric distribution of oxygen vacancies. *Phys. Rev. B* **82**, 125412 (2010).
30. Zhong, Z., Xu, P. X. & Kelly, P. J. Polarity-induiced oxygen vacancies at LAO/STO interfaces. *Phys. Rev. B* **82**, 165127 (2010).
31. Kresse, G. & Hafner, J. Ab initio molecular dynamics for liquid metals. *Phys. Rev. B* **47**, 558 (1993).
32. Perdew, J. P., Burke, K. & Ernzerhof, M. Generalized Gradient Approximation Made Simple. *Phys. Rev. Lett.* **77**, 3865 (1996).
33. Pentcheva, R. & Pickett, W. E. Charge localization or itineracy at LaAlO3/SrTiO3 interfaces: Hole polarons, oxygen vacancies, and mobile electrons. *Phys. Rev. B* **74**, 035112 (2006).
34. Son, W.-J., Cho, E., Lee, B., Lee, J. & Han, S. Density and spatial distribution of charge carriers in the intrinsic n-type LaAlO3-SrTiO3 interface. *Phys. Rev. B* **79**, 245411 (2009).
35. Wang, X. J., Xiao, H. Y., Zu, X. T., Zhang, Y. & Weber, W. J. Ab initio molecular dynamics simulations of ion–solid interactions in Gd2Zr2O7 and Gd2Ti2O7. *J. Mater. Chem. C* **1**, 1665 (2013).
36. Gao, F., Xiao, H. Y., Zu, X. T., Posselt, M. & Weber, W. J. Defect-Enhanced Charge Transfer by Ion-Solid Interactions in SiC using Large-Scale Ab Initio Molecular Dynamics Simulations. *Phys. Rev. Letts.* **103**, 027405 (2009).
37. Xiao, H. Y., Zhang, Y. & Weber, W. J. Ab initio molecular dynamics simulations of low-energy recoil events in ThO2, CeO2, and ZrO2. *Phys. Rev. B* **86**, 054109 (2012).
38. Xiao, H. Y., Gao, F. & Weber, W. J. Threshold displacement energies and defect formation energies in Y2Ti2O7. *J. Phys.: Condens Matter.* **22**, 415801 (2009).
39. Xiao, H. Y., Zhang, Y. & Weber, W. J. Stability and migration of charged oxygen interstitials in ThO2 and CeO2. *Acta. Mater.* **61**, 7639 (2013).
40. Vonk, V. *et al.* Interface structure of SrTiO3/LaAlO3 at elevated temperatures studied in situ by synchrotron x rays. *Phys. Rev. B* **75**, 235417 (2007).
41. Cen, C. *et al.* Nanoscale control of an interfacial metal–insulator transition at room temperature. *Nat. Mater.* **7**, 298 (2008).

Acknowledgments

X. Xiang and X.T. Zu were supported by the NSAF Joint Foundations of China (Grant No. U1330103 and U1230124) and Ph.D. Funding Support Program of Education Ministry of China (20110185110007). H.Y. Xiao acknowledges the scientific research starting funding of University of Electronic Science and Technology of China (Grant No. Y02002010401085).

Author contributions

X.Z., S.L. and W.Z. designed the calculations. H.X. and F.G. conducted the calculations. X.X. and L.Q. wrote the manuscript and prepared figures 1–5. All authors discussed the results and reviewed the manuscript.

Additional information

Competing financial interests: The authors declare no competing financial interests.

How to cite this article: Xiang, X. *et al.* Effects of surface defects on two-dimensional electron gas at $NdAlO_3/SrTiO_3$ interface. *Sci. Rep.* **4**, 5477; DOI:10.1038/srep05477 (2014).